

Search for $h_c \rightarrow \pi^+ \pi^- J/\psi$ via $\psi(3686) \rightarrow \pi^0 \pi^+ \pi^- J/\psi$

M. Ablikim,¹ M. N. Achasov,^{9,d} S. Ahmed,¹⁴ X. C. Ai,¹ M. Albrecht,⁴ D. J. Ambrose,⁴⁵ A. Amoroso,^{50a,50c} F. F. An,¹ Q. An,^{38,47} J. Z. Bai,¹ O. Bakina,²³ R. Baldini Ferroli,^{20a} Y. Ban,³¹ D. W. Bennett,¹⁹ J. V. Bennett,⁵ N. Berger,²² M. Bertani,^{20a} D. Bettoni,^{21a} J. M. Bian,⁴⁴ F. Bianchi,^{50a,50c} E. Boger,^{23,b} I. Boyko,²³ R. A. Briere,⁵ H. Cai,⁵² X. Cai,^{1,38} O. Cakir,^{41a} A. Calcaterra,^{20a} G. F. Cao,^{1,42} S. A. Cetin,^{41b} J. Chai,^{50c} J. F. Chang,^{1,38} G. Chelkov,^{23,b,c} G. Chen,¹ H. S. Chen,^{1,42} J. C. Chen,¹ M. L. Chen,^{1,38} P. L. Chen,⁴⁸ S. J. Chen,²⁹ X. R. Chen,²⁶ Y. B. Chen,^{1,38} X. K. Chu,³¹ G. Cibinetto,^{21a} H. L. Dai,^{1,38} J. P. Dai,^{34,h} A. Dbeysi,¹⁴ D. Dedovich,²³ Z. Y. Deng,¹ A. Denig,²² I. Denysenko,²³ M. Destefanis,^{50a,50c} F. De Mori,^{50a,50c} Y. Ding,²⁷ C. Dong,³⁰ J. Dong,^{1,38} L. Y. Dong,^{1,42} M. Y. Dong,¹ Z. L. Dou,²⁹ S. X. Du,⁵⁴ P. F. Duan,¹ J. Fang,^{1,38} S. S. Fang,^{1,42} Y. Fang,¹ R. Farinelli,^{21a,21b} L. Fava,^{50b,50c} S. Fegan,²² F. Feldbauer,²² G. Felici,^{20a} C. Q. Feng,^{38,47} E. Fioravanti,^{21a} M. Fritsch,^{14,22} C. D. Fu,¹ Q. Gao,¹ X. L. Gao,^{38,47} Y. Gao,⁴⁰ Z. Gao,^{38,47} I. Garzia,^{21a} K. Goetzen,¹⁰ L. Gong,³⁰ W. X. Gong,^{1,38} W. Gradl,²² M. Greco,^{50a,50c} M. H. Gu,^{1,38} Y. T. Gu,¹² A. Q. Guo,¹ R. P. Guo,^{1,42} Y. P. Guo,²² Z. Haddadi,²⁵ S. Han,⁵² X. Q. Hao,¹⁵ F. A. Harris,⁴³ K. L. He,^{1,42} X. Q. He,⁴⁶ F. H. Heinsius,⁴ T. Held,⁴ Y. K. Heng,¹ T. Holtmann,⁴ Z. L. Hou,¹ H. M. Hu,^{1,42} T. Hu,¹ Y. Hu,¹ G. S. Huang,^{38,47} J. S. Huang,¹⁵ X. T. Huang,³³ X. Z. Huang,²⁹ Z. L. Huang,²⁷ T. Hussain,⁴⁹ W. Ikegami Andersson,⁵¹ Q. Ji,¹ Q. P. Ji,¹⁵ X. B. Ji,^{1,42} X. L. Ji,^{1,38} L. W. Jiang,⁵² X. S. Jiang,¹ X. Y. Jiang,³⁰ J. B. Jiao,³³ Z. Jiao,¹⁷ Q. L. Jie,⁵² D. P. Jin,¹ S. Jin,^{1,42} T. Johansson,⁵¹ A. Julin,⁴⁴ N. Kalantar-Nayestanaki,²⁵ X. L. Kang,¹ X. S. Kang,³⁰ M. Kavatsyuk,²⁵ B. C. Ke,⁵ P. Kiese,²² R. Kliemt,¹⁰ B. Kloss,²² O. B. Kolcu,^{41b,f} B. Kopf,⁴ M. Kornicer,⁴³ A. Kupsc,⁵¹ W. Kühn,²⁴ J. S. Lange,²⁴ M. Lara,¹⁹ P. Larin,¹⁴ L. Lavezzi,^{50c,1} H. Leithoff,²² C. Leng,^{50c} C. Li,⁵¹ Cheng Li,^{38,47} D. M. Li,⁵⁴ F. Li,^{1,38} F. Y. Li,³¹ G. Li,¹ H. B. Li,^{1,42} H. J. Li,^{1,42} J. C. Li,¹ Jin Li,³² Kang Li,¹³ Ke Li,³³ Lei Li,³ P. L. Li,^{38,47} P. R. Li,^{7,42} Q. Y. Li,³³ W. D. Li,^{1,42} W. G. Li,¹ X. L. Li,³³ X. N. Li,^{1,38} X. Q. Li,³⁰ Z. B. Li,³⁹ H. Liang,^{38,47} Y. F. Liang,³⁶ Y. T. Liang,²⁴ G. R. Liao,¹¹ D. X. Lin,¹⁴ B. Liu,^{34,h} B. J. Liu,¹ C. X. Liu,¹ D. Liu,^{38,47} F. H. Liu,³⁵ Fang Liu,¹ Feng Liu,⁶ H. B. Liu,¹² H. M. Liu,^{1,42} Huanhuan Liu,¹ Huihui Liu,¹⁶ J. B. Liu,^{38,47} J. P. Liu,⁵² J. Y. Liu,^{1,42} K. Liu,⁴⁰ K. Y. Liu,²⁷ L. D. Liu,³¹ P. L. Liu,^{1,38} Q. Liu,⁴² S. B. Liu,^{38,47} X. Liu,²⁶ Y. B. Liu,³⁰ Z. A. Liu,¹ Zhiqing Liu,²² H. Loehner,²⁵ Y. F. Long,³¹ X. C. Lou,¹ H. J. Lu,¹⁷ J. G. Lu,^{1,38} Y. Lu,¹ Y. P. Lu,^{1,38} C. L. Luo,²⁸ M. X. Luo,⁵³ T. Luo,⁴³ X. L. Luo,^{1,38} X. R. Lyu,⁴² F. C. Ma,²⁷ H. L. Ma,¹ L. L. Ma,³³ M. M. Ma,^{1,42} Q. M. Ma,¹ T. Ma,¹ X. N. Ma,³⁰ X. Y. Ma,^{1,38} Y. M. Ma,³³ F. E. Maas,¹⁴ M. Maggiora,^{50a,50c} Q. A. Malik,⁴⁹ Y. J. Mao,³¹ Z. P. Mao,¹ S. Marcello,^{50a,50c} J. G. Messchendorp,²⁵ G. Mezzadri,^{21b} J. Min,^{1,38} T. J. Min,¹ R. E. Mitchell,¹⁹ X. H. Mo,¹ Y. J. Mo,⁶ C. Morales Morales,¹⁴ N. Yu. Muchnoi,^{9,d} H. Muramatsu,⁴⁴ P. Musiol,⁴ Y. Nefedov,²³ F. Nerling,¹⁰ I. B. Nikolaev,^{9,d} Z. Ning,^{1,38} S. Nisar,⁸ S. L. Niu,^{1,38} X. Y. Niu,^{1,42} S. L. Olsen,^{32,j} Q. Ouyang,¹ S. Pacetti,^{20b} Y. Pan,^{38,47} M. Papenbrock,⁵¹ P. Patteri,^{20a} M. Pelizaeus,⁴ H. P. Peng,^{38,47} K. Peters,^{10,g} J. Pettersson,⁵¹ J. L. Ping,²⁸ R. G. Ping,^{1,42} R. Poling,⁴⁴ V. Prasad,¹ H. R. Qi,² M. Qi,²⁹ S. Qian,^{1,38} C. F. Qiao,⁴² J. J. Qin,⁴² N. Qin,⁵² X. S. Qin,¹ Z. H. Qin,^{1,38} J. F. Qiu,¹ K. H. Rashid,^{49,i} C. F. Redmer,²² M. Ripka,²² G. Rong,^{1,42} Ch. Rosner,¹⁴ A. Sarantsev,^{23,e} M. Savrié,^{21b} C. Schmier,⁴ K. Schoenning,⁵¹ W. Shan,³¹ M. Shao,^{38,47} C. P. Shen,² P. X. Shen,³⁰ X. Y. Shen,^{1,42} H. Y. Sheng,¹ J. J. Song,³³ W. M. Song,³³ X. Y. Song,¹ S. Sosio,^{50a,50c} S. Spataro,^{50a,50c} G. X. Sun,¹ J. F. Sun,¹⁵ S. S. Sun,^{1,42} X. H. Sun,¹ Y. J. Sun,^{38,47} Y. Z. Sun,¹ Z. J. Sun,^{1,38} Z. T. Sun,¹⁹ C. J. Tang,³⁶ X. Tang,¹ I. Tapan,^{41c} E. H. Thorndike,⁴⁵ M. Tiemens,²⁵ I. Uman,^{41d} G. S. Varner,⁴³ B. Wang,¹ B. L. Wang,⁴² D. Wang,³¹ D. Y. Wang,³¹ Dan Wang,⁴² K. Wang,^{1,38} L. L. Wang,¹ L. S. Wang,¹ M. Wang,³³ P. Wang,¹ P. L. Wang,¹ W. P. Wang,^{38,47} X. F. Wang,⁴⁰ Y. Wang,³⁷ Y. D. Wang,¹⁴ Y. F. Wang,¹ Y. Q. Wang,²² Z. Wang,^{1,38} Z. G. Wang,^{1,38} Z. Y. Wang,¹ Zongyuan Wang,^{1,42} T. Weber,²² D. H. Wei,¹¹ P. Weidenkaff,²² S. P. Wen,¹ U. Wiedner,⁴ M. Wolke,⁵¹ L. H. Wu,¹ L. J. Wu,^{1,42} Z. Wu,^{1,38} L. Xia,^{38,47} Y. Xia,¹⁸ D. Xiao,¹ H. Xiao,⁴⁸ Z. J. Xiao,²⁸ Y. G. Xie,^{1,38} Y. H. Xie,⁶ X. A. Xiong,^{1,42} Q. L. Xiu,^{1,38} G. F. Xu,¹ J. J. Xu,^{1,42} L. Xu,¹ Q. J. Xu,¹³ Q. N. Xu,⁴² X. P. Xu,³⁷ L. Yan,^{50a,50c} W. B. Yan,^{38,47} Y. H. Yan,¹⁸ H. J. Yang,^{34,h} H. X. Yang,¹ L. Yang,⁵² Y. X. Yang,¹¹ M. Ye,^{1,38} M. H. Ye,⁷ J. H. Yin,¹ Z. Y. You,³⁹ B. X. Yu,¹ C. X. Yu,³⁰ J. S. Yu,²⁶ C. Z. Yuan,^{1,42} Y. Yuan,¹ A. Yuncu,^{41b,a} A. A. Zafar,⁴⁹ Y. Zeng,¹⁸ Z. Zeng,^{38,47} B. X. Zhang,¹ B. Y. Zhang,^{1,38} C. C. Zhang,¹ D. H. Zhang,¹ H. H. Zhang,³⁹ H. Y. Zhang,^{1,38} J. Zhang,^{1,42} J. L. Zhang,¹ J. Q. Zhang,¹ J. W. Zhang,¹ J. Y. Zhang,¹ J. Z. Zhang,^{1,42} K. Zhang,^{1,42} S. Q. Zhang,³⁰ X. Y. Zhang,³³ Y. H. Zhang,^{1,38} Y. T. Zhang,^{38,47} Yang Zhang,¹ Yao Zhang,¹ Yu Zhang,⁴² Z. H. Zhang,⁶ Z. P. Zhang,⁴⁷ Z. Y. Zhang,⁵² G. Zhao,¹ J. W. Zhao,^{1,38} J. Y. Zhao,^{1,42} J. Z. Zhao,^{1,38} Lei Zhao,^{38,47} Ling Zhao,¹ M. G. Zhao,³⁰ Q. Zhao,¹ S. J. Zhao,⁵⁴ T. C. Zhao,¹ Y. B. Zhao,^{1,38} Z. G. Zhao,^{38,47} A. Zhemchugov,^{23,b} B. Zheng,⁴⁸ J. P. Zheng,^{1,38} Y. H. Zheng,⁴² B. Zhong,²⁸ L. Zhou,^{1,38} X. Zhou,⁵² X. K. Zhou,^{38,47} X. R. Zhou,^{38,47} X. Y. Zhou,¹ J. Zhu,³⁰ K. Zhu,¹ K. J. Zhu,¹ S. Zhu,¹ S. H. Zhu,⁴⁶ X. L. Zhu,⁴⁰ Y. C. Zhu,^{38,47} Y. S. Zhu,^{1,42} Z. A. Zhu,^{1,42} J. Zhuang,^{1,38} L. Zotti,^{50a,50c} B. S. Zou,¹ and J. H. Zou¹

(BESIII Collaboration)

- ¹*Institute of High Energy Physics, Beijing 100049, People's Republic of China*
²*Beihang University, Beijing 100191, People's Republic of China*
³*Beijing Institute of Petrochemical Technology, Beijing 102617, People's Republic of China*
⁴*Bochum Ruhr-University, D-44780 Bochum, Germany*
⁵*Carnegie Mellon University, Pittsburgh, Pennsylvania 15213, USA*
⁶*Central China Normal University, Wuhan 430079, People's Republic of China*
⁷*China Center of Advanced Science and Technology, Beijing 100190, People's Republic of China*
⁸*COMSATS Institute of Information Technology,
Lahore, Defence Road, Off Raiwind Road, 54000 Lahore, Pakistan*
⁹*G. I. Budker Institute of Nuclear Physics SB RAS (BINP), Novosibirsk 630090, Russia*
¹⁰*GSI Helmholtzcentre for Heavy Ion Research GmbH, D-64291 Darmstadt, Germany*
¹¹*Guangxi Normal University, Guilin 541004, People's Republic of China*
¹²*Guangxi University, Nanning 530004, People's Republic of China*
¹³*Hangzhou Normal University, Hangzhou 310036, People's Republic of China*
¹⁴*Helmholtz Institute Mainz, Johann-Joachim-Becher-Weg 45, D-55099 Mainz, Germany*
¹⁵*Henan Normal University, Xinxiang 453007, People's Republic of China*
¹⁶*Henan University of Science and Technology, Luoyang 471003, People's Republic of China*
¹⁷*Huangshan College, Huangshan 245000, People's Republic of China*
¹⁸*Hunan University, Changsha 410082, People's Republic of China*
¹⁹*Indiana University, Bloomington, Indiana 47405, USA*
^{20a}*INFN Laboratori Nazionali di Frascati, I-00044 Frascati, Italy*
^{20b}*INFN and University of Perugia, I-06100 Perugia, Italy*
^{21a}*INFN Sezione di Ferrara, I-44122 Ferrara, Italy*
^{21b}*University of Ferrara, I-44122 Ferrara, Italy*
²²*Johannes Gutenberg University of Mainz, Johann-Joachim-Becher-Weg 45, D-55099 Mainz, Germany*
²³*Joint Institute for Nuclear Research, 141980 Dubna, Moscow region, Russia*
²⁴*Justus-Liebig-Universitaet Giessen, II. Physikalisches Institut, Heinrich-Buff-Ring 16,
D-35392 Giessen, Germany*
²⁵*KVI-CART, University of Groningen, NL-9747 AA Groningen, The Netherlands*
²⁶*Lanzhou University, Lanzhou 730000, People's Republic of China*
²⁷*Liaoning University, Shenyang 110036, People's Republic of China*
²⁸*Nanjing Normal University, Nanjing 210023, People's Republic of China*
²⁹*Nanjing University, Nanjing 210093, People's Republic of China*
³⁰*Nankai University, Tianjin 300071, People's Republic of China*
³¹*Peking University, Beijing 100871, People's Republic of China*
³²*Seoul National University, Seoul 151-747, Korea*
³³*Shandong University, Jinan 250100, People's Republic of China*
³⁴*Shanghai Jiao Tong University, Shanghai 200240, People's Republic of China*
³⁵*Shanxi University, Taiyuan 030006, People's Republic of China*
³⁶*Sichuan University, Chengdu 610064, People's Republic of China*
³⁷*Soochow University, Suzhou 215006, People's Republic of China*
³⁸*State Key Laboratory of Particle Detection and Electronics,
Beijing 100049, Hefei 230026, People's Republic of China*
³⁹*Sun Yat-Sen University, Guangzhou 510275, People's Republic of China*
⁴⁰*Tsinghua University, Beijing 100084, People's Republic of China*
^{41a}*Ankara University, 06100 Tandogan, Ankara, Turkey*
^{41b}*Istanbul Bilgi University, 34060 Eyup, Istanbul, Turkey*
^{41c}*Uludag University, 16059 Bursa, Turkey*
^{41d}*Near East University, Nicosia, 99138 North Cyprus, Mersin 10, Turkey*
⁴²*University of Chinese Academy of Sciences, Beijing 100049, People's Republic of China*
⁴³*University of Hawaii, Honolulu, Hawaii 96822, USA*
⁴⁴*University of Minnesota, Minneapolis, Minnesota 55455, USA*
⁴⁵*University of Rochester, Rochester, New York 14627, USA*
⁴⁶*University of Science and Technology Liaoning, Anshan 114051, People's Republic of China*
⁴⁷*University of Science and Technology of China, Hefei 230026, People's Republic of China*
⁴⁸*University of South China, Hengyang 421001, People's Republic of China*
⁴⁹*University of the Punjab, Lahore 54590, Pakistan*
^{50a}*University of Turin, I-10125 Turin, Italy*
^{50b}*University of Eastern Piedmont, I-15121 Alessandria, Italy*
^{50c}*INFN, I-10125 Turin, Italy*

⁵¹*Uppsala University, Box 516, SE-75120 Uppsala, Sweden*⁵²*Wuhan University, Wuhan 430072, People's Republic of China*⁵³*Zhejiang University, Hangzhou 310027, People's Republic of China*⁵⁴*Zhengzhou University, Zhengzhou 450001, People's Republic of China*

(Received 11 January 2018; published 23 March 2018)

Using a data sample of 448.1×10^6 $\psi(3686)$ events collected with the BESIII detector operating at the BEPCII, we perform search for the hadronic transition $h_c \rightarrow \pi^+\pi^-J/\psi$ via $\psi(3686) \rightarrow \pi^0 h_c$. No signals of the transition are observed, and the upper limit on the product branching fraction $\mathcal{B}(\psi(3686) \rightarrow \pi^0 h_c) \mathcal{B}(h_c \rightarrow \pi^+\pi^-J/\psi)$ at the 90% confidence level (C.L.) is determined to be 2.0×10^{-6} . This is the most stringent upper limit to date.

DOI: [10.1103/PhysRevD.97.052008](https://doi.org/10.1103/PhysRevD.97.052008)

I. INTRODUCTION

Heavy quarkonium ($Q\bar{Q}$) presents an ideal environment for testing the interplay between perturbative and non-perturbative quantum chromodynamics (QCD) [1]. Hadronic transitions between the heavy $Q\bar{Q}$ states are particularly interesting. A common approach for calculating these transitions is the QCD multipole expansion (QCDME) [2] for gluon emission. The calculation depends on experimental inputs and works well for transitions of heavy $Q\bar{Q}$ states below open flavor threshold [3]. But some puzzles remain to pose challenge to the theory. For example, the measured ratio $\frac{\Gamma(Y(2S) \rightarrow \eta Y(1S))}{\Gamma(\psi(2S) \rightarrow \eta J/\psi)}$ [4] is much smaller than the theoretical prediction. Hence, more experimental measurements for the transition of heavy $Q\bar{Q}$ are desirable to constrain and challenge the theory models. However to

date, the only well-measured hadronic transitions in the charmonium sector are those for the $\psi(3686)$.

For charmonium states below the $D\bar{D}$ threshold, the hadronic transitions of the spin-singlet P-wave state $h_c(1^1P_1)$ are one of the best places to test the spin-spin interaction between heavy quarks [5], but they remain the least accessible experimentally because the $h_c(1^1P_1)$ cannot be produced resonantly in e^+e^- annihilation or from electric-dipole radiative transitions of the $\psi(3686)$. Evidence for the h_c state was reported in $p\bar{p} \rightarrow h_c \rightarrow \gamma\eta_c$ by E835 [6] at Fermilab. The first observation of the h_c was reported by CLEO in a study of the cascade decay $\psi(3686) \rightarrow \pi^0 h_c, h_c \rightarrow \gamma\eta_c$ [7]. With large statistics, CLEO measured the h_c mass precisely [8], and presented evidence for multi-pion decay modes [9], which imply that the h_c state has comparable rates for the decay to hadronic final states and the radiative transition to the η_c state. Furthermore, for the first time the BESIII Collaboration measured the branching fractions $\mathcal{B}(\psi(3686) \rightarrow \pi^0 h_c) = (8.4 \pm 1.3 \pm 1.0) \times 10^{-4}$ and $\mathcal{B}(h_c \rightarrow \gamma\eta_c) = (54.3 \pm 6.7 \pm 5.2)\%$ [10], which were confirmed by CLEO [11].

The h_c is also expected to decay to lower-mass charmonia state through hadronic transitions, but this has not been observed yet. In the framework of QCDME, the branching fraction of $h_c \rightarrow \pi\pi J/\psi$ (including charged and neutral modes) is predicted to be 2% [12], while it is predicted to be 0.05% when neglecting the nonlocality in time [13]. An experimental measurement is desirable to distinguish between these calculations. In this paper, we perform a search for the hadronic transition $h_c \rightarrow \pi^+\pi^-J/\psi$ using a data sample consisting of (448.1 ± 2.9) million $\psi(3686)$ events [14] collected at a center-of-mass energy of 3.686 GeV, corresponding to the peak of $\psi(3686)$ resonance. Considering kinematic limitation and parity conservation, the angular momentum between the two-pion system (in a relative S-wave) and J/ψ should be P-wave, and the transition rate of $h_c \rightarrow \pi^+\pi^-J/\psi$ is suppressed. Thus, statistical limitation and low detection efficiency for the soft pions are the two major challenges to study $h_c \rightarrow \pi^+\pi^-J/\psi$. Taking into account the theoretically

^aAlso at Bogazici University, 34342 Istanbul, Turkey.^bAlso at the Moscow Institute of Physics and Technology, Moscow 141700, Russia.^cAlso at the Functional Electronics Laboratory, Tomsk State University, Tomsk, 634050, Russia.^dAlso at the Novosibirsk State University, Novosibirsk, 630090, Russia.^eAlso at the NRC “Kurchatov Institute”, PNPI, 188300, Gatchina, Russia.^fAlso at Istanbul Arel University, 34295 Istanbul, Turkey.^gAlso at Goethe University Frankfurt, 60323 Frankfurt am Main, Germany.^hAlso at Key Laboratory for Particle Physics, Astrophysics and Cosmology, Ministry of Education; Shanghai Key Laboratory for Particle Physics and Cosmology; Institute of Nuclear and Particle Physics, Shanghai 200240, People's Republic of China.ⁱGovernment College Women University, Sialkot—51310. Punjab, Pakistan.^jPresent address: Center for Underground Physics, Institute for Basic Science, Daejeon 34126, Korea.

predicted branching fraction for transition $h_c \rightarrow \pi^+ \pi^- J/\psi$, the other related decay branching fractions from Particle Data Group (PDG) [15] and the total number of $\psi(3686)$ used in this analysis and without consideration of detection efficiency, the signal yield of $\psi(3686) \rightarrow \pi^0 h_c, \pi^0 \rightarrow \gamma\gamma, h_c \rightarrow \pi^+ \pi^- J/\psi, J/\psi \rightarrow l^+ l^- (l = e, \mu)$ is expected to be 600 and 15 for the predictions of Refs. [12,13], respectively.

This paper is structured as follows: in Sec. II the BESIII detector is described and details of the Monte Carlo (MC) samples are given. In Sec. III, the analysis strategy, event selection criteria and background analysis are introduced. Section IV presents the estimation of the upper limit, and Sec. V provides the systematic uncertainties of the measurement. Finally, a short summary and a discussion of the result are given in Sec. VI.

II. BESIII DETECTOR AND MONTE CARLO SIMULATION

The BESIII detector is designed to facilitate physics research in the τ -charm region in e^+e^- annihilations with center-of-mass energies from 2 to 4.6 GeV at the Beijing Electron Positron Collider II (BEPCII). The detector has a geometric acceptance of 93% of the solid angle and mainly consists of five components: (1) a helium-gas-based main drift chamber (MDC) for tracking and particle identification using the specific energy loss dE/dx . The expected charged particle momentum resolution at 1 GeV and dE/dx resolution are 0.5% and 6%, respectively. (2) a plastic scintillator time-of-flight system with an intrinsic time resolution of 80 ps in the barrel region and 110 ps in the end-cap region. (3) a CsI(Tl) crystal calorimeter (EMC) with an energy resolution better than 2.5% in the barrel region and 5% in the end-cap region, and a position resolution better than 6 mm for 1 GeV electrons and photons. (4) a superconductive solenoid magnet with a central field of 1.0 Tesla. (5) a muon chamber system composed of nine barrel layers and eight end-cap layers of resistive plate chambers with a spatial resolution better than 2 cm. More details on the construction and capabilities of BESIII detector may be found in Ref. [16].

The optimization of event selection criteria, study of backgrounds and determination of detection efficiency are based on samples of MC simulated events. A GEANT4-based [17] software is used to describe the geometry of the BESIII detector and simulate the detector response. A MC sample of 506 million generic $\psi(3686)$ decays ('inclusive MC sample') is generated to study the background processes. The $\psi(3686)$ resonance is generated by KKMC [18] with final state radiation (FSR) effects handled with PHOTOS [19]. The known decay modes are generated by EvtGen [20] with branching fractions set to the world average values according to the PDG [21]; the remaining unknown charmonium decays are generated with LundCharm [22]. The signal channel

$\psi(3686) \rightarrow \pi^0 h_c, h_c \rightarrow \pi^+ \pi^- J/\psi$ is excluded from the inclusive sample.

The signal MC sample of $\psi(3686) \rightarrow \pi^0 h_c, h_c \rightarrow \pi^+ \pi^- J/\psi$ is generated uniformly in phase space with the π^0 decaying to two photons and the J/ψ decaying to $l^+ l^- (l = e, \mu)$. The MC sample of $\psi(3686) \rightarrow \eta J/\psi$ with η decaying to $\pi^0 \pi^+ \pi^-$ and J/ψ decaying to $l^+ l^-$ is generated to study the background and determine the detection efficiency of this process. The angular distribution of the η is modeled as $1 + \cos^2 \theta_\eta$, where θ_η is the angle between η momentum and the positron beam in the rest frame of $\psi(3686)$. The decay $\eta \rightarrow \pi^0 \pi^+ \pi^-$ is generated by EvtGen [20] with the measured Dalitz plot amplitude [23], and $\pi^0 \rightarrow \gamma\gamma$ by a phase space distribution. The J/ψ decays to $l^+ l^-$ are generated with an angular distribution of $1 + \cos^2 \theta_l$, where θ_l is the angle between the l^+ momentum in the J/ψ rest frame and the J/ψ momentum in the $\psi(3686)$ rest frame.

III. METHODOLOGY AND EVENT SELECTION

A relative measurement strategy is used to measure $h_c \rightarrow \pi^+ \pi^- J/\psi$ according to

$$\mathcal{B}(\psi(3686) \rightarrow \pi^0 h_c) \mathcal{B}(h_c \rightarrow \pi^+ \pi^- J/\psi) = \frac{N_{\text{sig}}^{\text{obs}} \epsilon_{\text{ref}}}{N_{\text{ref}}^{\text{obs}} \epsilon_{\text{sig}}} \mathcal{B}(\psi(3686) \rightarrow \eta J/\psi) \mathcal{B}(\eta \rightarrow \pi^0 \pi^+ \pi^-). \quad (1)$$

The decay $\psi(3686) \rightarrow \pi^0 h_c \rightarrow \pi^0 \pi^+ \pi^- J/\psi$ is the signal mode, and the decay $\psi(3686) \rightarrow \eta J/\psi \rightarrow \pi^0 \pi^+ \pi^- J/\psi$, which has the same final state as the signal, serves as the reference mode. These two processes will be selected simultaneously. Then the product $\mathcal{B}(\psi(3686) \rightarrow \pi^0 h_c) \mathcal{B}(h_c \rightarrow \pi^+ \pi^- J/\psi)$ can be obtained by the ratio of the numbers of observed events $N_{\text{sig}}^{\text{obs}}/N_{\text{ref}}^{\text{obs}}$ and the ratio of detection efficiencies $\epsilon_{\text{ref}}/\epsilon_{\text{sig}}$ of these two processes. With this relative measurement method, most of the systematic uncertainties in the efficiencies and that of the total number of $\psi(3686)$ events cancel.

Charged tracks are reconstructed from hits in the MDC and are required to originate from the interaction point, i.e., passing within 10 cm to the interaction point in the beam direction and 1 cm in the plane perpendicular to the beam. In addition, the polar angle θ of each track is required to satisfy $|\cos \theta| < 0.93$. Electromagnetic showers are reconstructed from clusters in the EMC. A good photon candidate is an isolated shower that is required to have energy larger than 25 MeV in the barrel region of the EMC ($|\cos \theta| < 0.8$) or 50 MeV in the end-cap regions ($0.86 < |\cos \theta| < 0.92$). Showers in the transition region between the barrel and the end-cap are removed since they are not well reconstructed. In addition, timing information from the EMC ($0 \leq t \leq 700$ ns) is used to suppress electronic noise and energy deposits unrelated to the event.

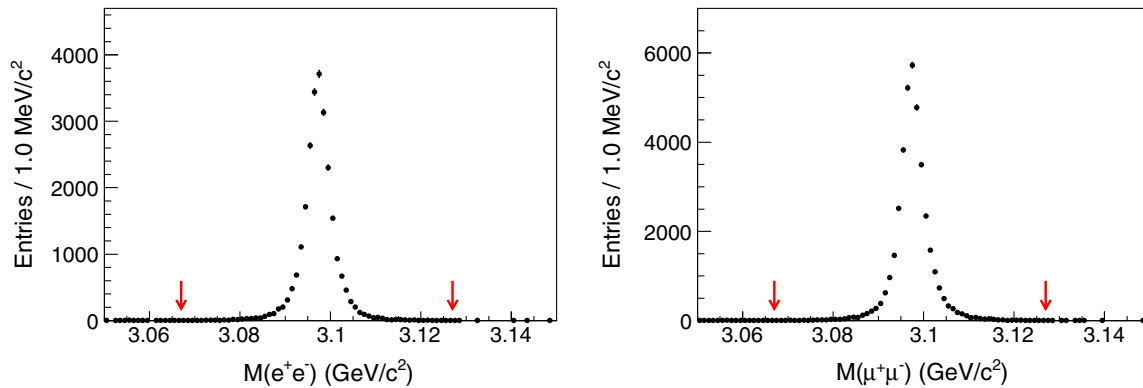


FIG. 1. Distributions of $M(e^+e^-)$ (left) and $M(\mu^+\mu^-)$ (right) in data. The arrows show the signal region.

For events of interest, including $\psi(3686) \rightarrow \pi^0 h_c$, $h_c \rightarrow \pi^+\pi^-J/\psi$ (signal mode), and $\psi(3686) \rightarrow \eta J/\psi$, $\eta \rightarrow \pi^0\pi^+\pi^-$ (reference mode), we require that there are four good charged tracks with zero net charge and at least two good photon candidates. The track momentum is used to separate leptons and pions since the momenta of leptons from J/ψ decay are higher than 1 GeV/c. Charged tracks with momenta less than 1 GeV/c are assumed to be pions, while the remaining two tracks are taken as leptons. Electrons and muons are identified according to the ratio of energy (E) deposited in the EMC and momentum (p) measured in MDC. Tracks with $E/pc > 0.7$ are taken as electrons, and those with $E/pc < 0.3$ are identified as muons. A pair of pions with opposite charge and a pair of leptons with same flavor and opposite charge are required. Photon pairs with invariant mass in the region $120 < M(\gamma\gamma) < 145$ MeV/c² are combined into π^0 candidates. To avoid bias in choosing the best combination, all combinations due to multiple π^0 candidates are retained. Only 0.5% of all events contain more than one π^0 candidate, and this is modeled well in the simulation. The $\pi^+\pi^-$ invariant mass $M(\pi^+\pi^-)$ should be larger than 0.3 GeV/c² to reject backgrounds from $\pi^0\pi^0J/\psi$ with γ converting into an e^+e^- pair in the beam pipe or inner wall of the MDC.

A five-constraint (5C) kinematic fit is performed for the $\pi^0\pi^+\pi^-l^+l^-$ combination enforcing energy and momentum conservation and constraining the invariant mass of the photon pair to the π^0 nominal mass [15]. Events with $\chi_{5C}^2 < 60$ are accepted for further analysis. After imposing these criteria, clear J/ψ peaks with low background levels are observed in both the e^+e^- and $\mu^+\mu^-$ invariant mass distributions, as shown in Fig. 1. For the selection of J/ψ candidates, the invariant mass of lepton pairs $M(l^+l^-)$ is required to be in the J/ψ mass region, i.e. $|M(l^+l^-) - M(J/\psi)| < 30$ MeV/c², where $M(J/\psi)$ is the nominal mass of the J/ψ [15].

Based on studies of the inclusive MC sample, the dominant surviving event candidates are from

$\psi(3686) \rightarrow \eta J/\psi$, $\eta \rightarrow \pi^0\pi^+\pi^-$, while background from events with different final states is negligible. A clear η peak with a low level of background is observed in the $\pi^0\pi^+\pi^-$ invariant mass spectrum, $M(\pi^0\pi^+\pi^-)$, as shown in Fig. 2.

In order to validate the event selection criteria, we calculate the branching fraction $\mathcal{B}(\psi(3686) \rightarrow \eta J/\psi)$ and compare it with a previous BESIII measurement [24], where η is reconstructed via two photons and only the first set of the data sample of (107.0 ± 0.8) million $\psi(3686)$ taken in 2009 [14] was used. In our calculation, the yield of $\psi(3686) \rightarrow \eta J/\psi$, $\eta \rightarrow \pi^0\pi^+\pi^-$ is obtained by counting events in the η signal region and subtracting the events in the η sideband region. The η signal region is defined as $|M(\pi^0\pi^+\pi^-) - M(\eta)| < 15$ MeV/c², where $M(\eta)$ is the η nominal mass [15]. It covers about 99.2% of the $\eta J/\psi$ signal according to the MC simulation. The η sideband region is defined as $30 < |M(\pi^0\pi^+\pi^-) - M(\eta)| < 45$ MeV/c². Using the same sample of 107 million $\psi(3686)$ events, we obtain $\mathcal{B}(\psi(3686) \rightarrow \eta J/\psi) = (33.89 \pm 0.27(\text{stat.})) \times 10^{-3}$, which is consistent with the previous measurement $(33.75 \pm 0.17(\text{stat.}) \pm 0.86(\text{syst.})) \times 10^{-3}$.

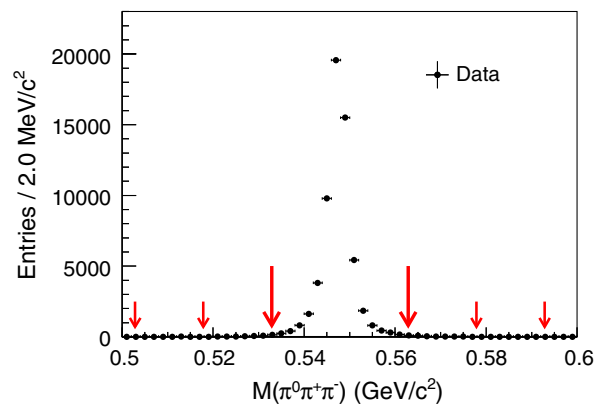


FIG. 2. Distribution of $M(\pi^0\pi^+\pi^-)$ of data, the longer red arrows indicate the signal region of $\psi(3686) \rightarrow \eta J/\psi$ and the shorter red arrows correspond to the sideband regions.

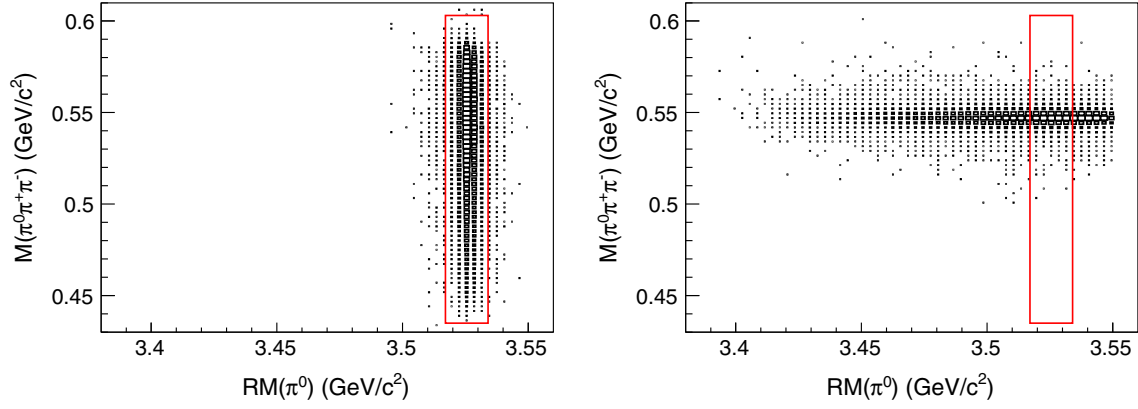


FIG. 3. Two-dimensional distributions of $M(\pi^0\pi^+\pi^-)$ versus $RM(\pi^0)$ for the signal MC sample (left) and data (right). The red box indicates the h_c signal region.

IV. UPPER LIMIT ON

$$\mathcal{B}(\psi(3686) \rightarrow \pi^0 h_c) \mathcal{B}(h_c \rightarrow \pi^+ \pi^- J/\psi)$$

The two-dimensional distributions of $M(\pi^0\pi^+\pi^-)$ versus the π^0 recoil mass $RM(\pi^0)$ for the signal MC sample and data are shown in Fig. 3, and the distribution of $RM(\pi^0)$ is shown in Fig. 4. To improve the resolution, $RM(\pi^0)$ is calculated using the four-momenta after constraining the invariant mass of the photon pair to the π^0 nominal mass [15] (1C). The process $\psi(3686) \rightarrow \eta J/\psi$ is clearly dominant, but no obvious signal events from $\psi(3686) \rightarrow \pi^0 h_c$, $h_c \rightarrow \pi^+ \pi^- J/\psi$ are observed.

In order to obtain the yield of the decay of interest, we veto $\psi(3686) \rightarrow \eta J/\psi$ by imposing the further requirement $|M(\pi^0\pi^+\pi^-) - M(\eta)| > 32 \text{ MeV}/c^2$. For $\psi(3686) \rightarrow \eta J/\psi$, events off the η peak region are those with bad resolution and large χ_{5C}^2 . Thus, to further suppress the events from $\psi(3686) \rightarrow \eta J/\psi$ which are far from the η signal region, a tighter requirement $\chi_{5C}^2 < 15$ is imposed. With the above

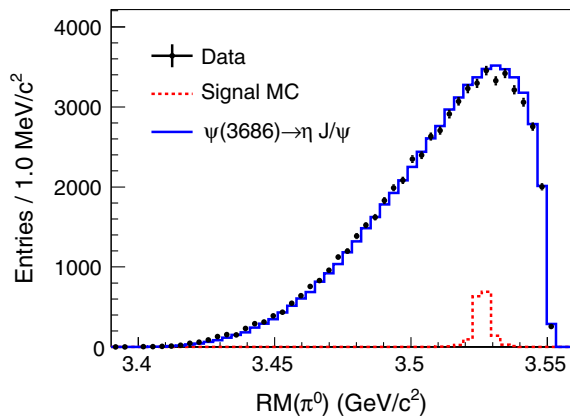


FIG. 4. Distribution of $RM(\pi^0)$ after the 1C kinematic fit. Black dots with error bars show data. The red dashed histogram shows the MC simulated signal shape (with arbitrary normalization). The blue solid histogram is the MC distribution of the reference mode.

requirements, 99.99% of the $\psi(3686) \rightarrow \eta J/\psi$ backgrounds are removed according to MC simulation. No events in data survive in the full region of $RM(\pi^0)$. Based on a study of the inclusive MC sample, there are only two background events from $\psi(3686) \rightarrow 2(\pi^+\pi^-)\pi^0$ left. Neither event is in the signal region of the h_c , which is defined as $3.517 < RM(\pi^0) < 3.534 \text{ GeV}/c^2$. We therefore take the expected number of observed background events $\bar{N}_{\text{bkg}}^{\text{obs}}$ in the signal region as zero. The upper limit on the number of observed signal events $N_{\text{sig}}^{\text{obs}}$ at the 90% C.L. is 2.44, which is estimated by using the Feldman-Cousins frequentist approach [25] without considering the systematic uncertainties. All the numbers used to extract the upper limit of signal yield are summarized in Table I. It is assumed that $N_{\text{sig}}^{\text{obs}}$ and $N_{\text{bkg}}^{\text{obs}}$ follow Poisson distributions. The number of events and the efficiency of the reference mode are obtained with the same method and requirements as in Sec. III, only with $\chi_{5C}^2 < 15$ instead of $\chi_{5C}^2 < 60$.

The upper limit on the product branching fraction $\mathcal{B}(\psi(3686) \rightarrow \pi^0 h_c) \mathcal{B}(h_c \rightarrow \pi^+ \pi^- J/\psi)$ at the 90% C.L.

TABLE I. Summary table. In order: upper limit on the number of observed signal events $(N_{\text{sig}}^{\text{obs}})^{\text{up}}$, the number of observed background events $N_{\text{bkg}}^{\text{obs}}$, signal efficiency (ϵ_{sig}), the number of observed events of reference mode ($N_{\text{ref}}^{\text{obs}}$), efficiency of reference mode (ϵ_{ref}), statistical uncertainty (σ^{stat}) and total uncertainty (σ^{tot}).

Quantity	Value
$(N_{\text{sig}}^{\text{obs}})^{\text{up}}$	2.44
$N_{\text{bkg}}^{\text{obs}}$	0
ϵ_{sig}	2.52%
$N_{\text{ref}}^{\text{obs}}$	31611 ± 178
ϵ_{ref}	8.25%
σ^{stat}	0.57%
σ^{tot}	15.4%

TABLE II. Summary of systematic uncertainties.

Sources	Systematic uncertainties (%)
$\mathcal{B}(\psi(3686) \rightarrow \eta J/\psi)$	1.5
$\mathcal{B}(\eta \rightarrow \pi^0\pi^+\pi^-)$	1.2
MC model	15.2
Total	15.4

is obtained by replacing $N_{\text{sig}}^{\text{obs}}$ in Eq. (1) with $(N_{\text{sig}}^{\text{obs}})^{\text{up}}(1 + (N_{\text{sig}}^{\text{obs}})^{\text{up}}(\sigma^{\text{tot}})^2/2)$ using the method proposed by Cousins and Highland [26] to incorporate the systematic uncertainty. The branching fractions of $\psi(3686) \rightarrow \eta J/\psi$ and $\eta \rightarrow \pi^0\pi^+\pi^-$ are taken from PDG [15]. The upper limit on $\mathcal{B}(\psi(3686) \rightarrow \pi^0 h_c)\mathcal{B}(h_c \rightarrow \pi^+\pi^-J/\psi)$ at the 90% C.L. is found to be 2.0×10^{-6} .

V. SYSTEMATIC UNCERTAINTY

In this analysis, the upper limit is obtained with a relative measurement strategy defined by Eq. (1). Since the signal mode and reference mode have same final states, and the uncertainty associated with the detection efficiency, i.e. trigger, photon detection, tracking and PID for charged tracks, π^0 reconstruction, and the 5C kinematic fit cancel. The systematic uncertainty due to the $M(\pi^0\pi^+\pi^-)$ resolution is less than 0.1% and is negligible.

The $M(\pi^+\pi^-)$ spectrum in the final state of $h_c \rightarrow \pi^+\pi^-J/\psi$ is unclear due to its unknown dynamics. In the nominal analysis, the signal MC sample is generated uniformly in the phase space without considering the angular distribution. In order to estimate the related uncertainties of the MC model, an alternative signal MC sample is generated by assuming a pure P-wave production between the two-pion system (S-wave) and J/ψ , where the production amplitude is proportional to the third power of the momentum of the $\pi^+\pi^-$ system. The difference in detection efficiency between the two MC samples, 15.2%, is taken as the systematic uncertainty associated with the MC model.

The branching fractions of $\psi(3686) \rightarrow \eta J/\psi$ and $\eta \rightarrow \pi^0\pi^+\pi^-$ are taken from the PDG [15]. The uncertainties of the branching fractions, 1.5% and 1.2%, are considered as systematic uncertainties. The individual systematic uncertainties are summarized in Table II. Assuming that all sources of systematic uncertainties are independent, a total systematic uncertainty of 15.4% is obtained by taking the quadratic sum of the individual contributions.

VI. SUMMARY

In summary, a search for the hadronic transition $h_c \rightarrow \pi^+\pi^-J/\psi$ is carried out via $\psi(3686) \rightarrow \pi^0 h_c, h_c \rightarrow \pi^+\pi^-J/\psi$.

No signal is observed. The upper limit of the product of branching fractions $\mathcal{B}(\psi(3686) \rightarrow \pi^0 h_c)\mathcal{B}(h_c \rightarrow \pi^+\pi^-J/\psi)$ at the 90% C.L. is determined to be 2.0×10^{-6} . Using the PDG value for the branching fraction of $\psi(3686) \rightarrow \pi^0 h_c$ of $(8.6 \pm 1.3) \times 10^{-4}$ [15], the upper limit on $\mathcal{B}(h_c \rightarrow \pi^+\pi^-J/\psi)$ is determined to be 2.4×10^{-3} , which is the most stringent upper limit to date. Neglecting the small phase space difference between the charged and neutral $\pi\pi$ modes and assuming isospin symmetry, we obtain $\mathcal{B}(h_c \rightarrow \pi\pi J/\psi) < 3.6 \times 10^{-3}$ (including charged and neutral modes) at the 90% C.L. It is noted that the measured branching fraction is smaller than the prediction in Ref. [12] by one order in magnitude, but does not contradict that in Ref. [13].

ACKNOWLEDGMENTS

The BESIII Collaboration thanks the staff of BEPCII and the IHEP computing center for their strong support. This work is supported in part by National Key Basic Research Program of China under Contract No. 2015CB856700; National Natural Science Foundation of China (NSFC) under Contracts No. 11205117, No. 11235011, No. 11322544, No. 11335008, No. 11425524, No. 11575133; the Chinese Academy of Sciences (CAS) Large-Scale Scientific Facility Program; the CAS Center for Excellence in Particle Physics (CCEPP); the Collaborative Innovation Center for Particles and Interactions (CICPI); Joint Large-Scale Scientific Facility Funds of the NSFC and CAS under Contracts No. U1232201, No. U1332201; CAS under Contracts No. KJCX2-YW-N29, No. KJCX2-YW-N45; 100 Talents Program of CAS; National 1000 Talents Program of China; INPAC and Shanghai Key Laboratory for Particle Physics and Cosmology; Hubei Nuclear Solid Physics Key Laboratory; German Research Foundation DFG under Contracts Nos. Collaborative Research Center CRC 1044, FOR 2359; Istituto Nazionale di Fisica Nucleare, Italy; Joint Large-Scale Scientific Facility Funds of the NSFC and CAS under Contract No. U1532257; Joint Large-Scale Scientific Facility Funds of the NSFC and CAS under Contract No. U1532258; Koninklijke Nederlandse Akademie van Wetenschappen (KNAW) under Contract No. 530-4CDP03; Ministry of Development of Turkey under Contract No. DPT2006K-120470; National Science and Technology fund; The Swedish Research Council; U.S. Department of Energy under Contracts No. DE-FG02-05ER41374, No. DE-SC-0010504, No. DE-SC0012069; U.S. National Science Foundation; University of Groningen (RuG) and the Helmholtzzentrum fuer Schwerionenforschung GmbH (GSI), Darmstadt; WCU Program of National Research Foundation of Korea under Contract No. R32-2008-000-10155-0.